Numerical Solution to Dynamic Timoshenko Beam with Uncertain Material and Forcing

Conor Rowan *
University of Colorado Boulder, Boulder, CO, 80303

A Timoshenko beam is a simplified model of the governing equations of linear elasticity which places fewer restrictions on the displacement field than the famous Euler beam model. In the Timoshenko model, a second unknown is introduced which allows the rotation of the cross-section to be independent of the transverse displacement. This accounts for shear deformations in bending, and is typically used in the analysis of thick beams. A dynamic analysis can be carried out with Hamilton's principle by introducing the appropriate translational and rotational kinetic energies. In this report, the governing equations of a dynamic Timoshenko beam with pinned boundary conditions are derived and solved approximately with the Rayleigh-Ritz method. The numerical solver is then used to quantify the influence of uncertain model parameters and inputs on a quantity of interest.

I. Introduction

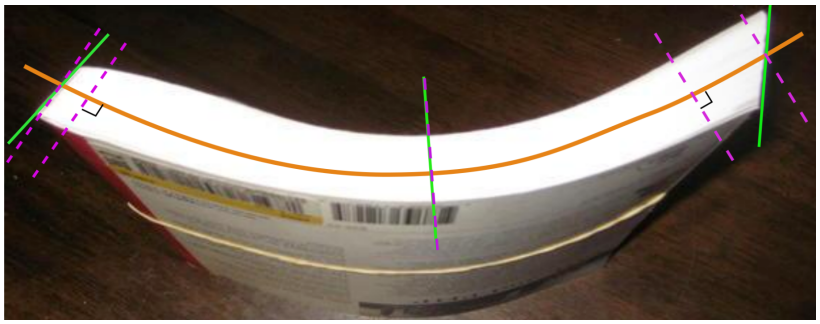

Fig. 1 A paperback book is an example of structure with very little resistance to shear deformations in bending. The purple line illustrates the angle of the cross-section enforced by Euler beam theory which assumes the cross-section remains perpendicular to the axis of the beam. The discrepancy between this and the actual cross-section shown in green indicates the necessity of incorporating shear effects. Borrowed from [1].

In the context of solid mechanics, a beam is a long, slender structure which displaces perpendicular to its axis under the action of applied loads. Because the length of a beam is much greater than its other two dimensions (depth and height), the elastic equations of equilibrium take a much simpler form, depending only on the spatial coordinate defined along the axis of the beam. Beam theories have been important in the history of structural analysis and engineering design because they offer insight into many structures of interest and often permit analytical solutions. For these reasons, beam theories were one of the mainstays of structural analysis before robust computational methods were widely available. The oldest beam theory dates back to the 1700's and is attributed to Euler. In this method, a single ODE for the bending displacement is obtained by neglecting shear effects in bending. In the early 1900's, Timoshenko contributed a new beam theory with a more general displacement. Because Timoshenko introduced a second unknown governing shear deformations, his theory resulted in the strong form of static equilibrium being governed by a system of coupled ODE's.

Though the Timoshenko beam theory furnishes a relationship between the beam's geometry, material parameters, applied forces and the bending displacement, this is not sufficient for real-world design or analysis problems. In practice, engineered structures are variable in their build (through material variability, manufacturing tolerances, etc) and load

*PhD Student, Aerospace Engineering

conditions. The idealized model does not capture the influence of these variations and therefore cannot prove that a structure will perform as desired in service [2]. For example, a candidate beam design might have an upper bound on the allowable bending stress. A deterministic analysis for a given force magnitude/location, material, or cross-sectional geometry could show that this threshold is not exceeded, but from the designers standpoint, these inputs are uncertain. It is imperative that the designer not only show that the design is compliant when tested in a deterministic way, but that it is safe when accounting for uncertainty in the inputs. Whereas universal physical principles are employed to construct a model, the language of probability is used to understand how uncertainty propagates through this model.

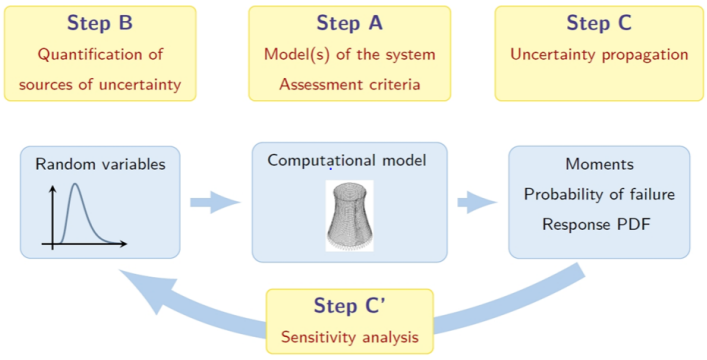

Fig. 2 Schematic of the analysis cycle for a typical engineering component. Once a model is constructed, variation in model inputs is captured with probability distributions, and this uncertainty is propagated through the model. Sensitivity analysis can then be used to determine which inputs contribute most to variation in the output. Borrowed from [3].

II. Motivation

This report is an effort to understand the various stages of a structural analysis problem through an example which is relevant to the Dynamics course and potential future work with uncertainty analysis in continuous systems. Broadly speaking, this comprises two main steps: model construction and uncertainty quantification (UQ). The Timoshenko beam is a canonical model in solid mechanics, and provides useful experience with foundational concepts such as kinematic assumptions, variational formulations, Rayleigh-Ritz method, and spectral solutions to MDOF systems. Once derived and implemented, the Timoshenko model is then used to illustrate the importance of understanding the propagation of uncertainty through the model. These two pillars of the project are beneficial from a pedagogical standpoint, but they also mirror analysis of a real-world engineered structure. See Figure 2.

III. Solution Approach

In the Timoshenko beam model, the rotation of the cross-section and the transverse displacements govern the bending problem and are independent parameters [4]. The assumed form of the displacement is

$$u_x = -y\Phi(x); \quad u_y = u(x); \quad u_z = 0 \tag{1}$$

The strain tensor ϵ can be computed using the infinitesimal strain-displacement relations with the Timoshenko kinematic assumptions. The only non-zero strain components are

$$\epsilon_{xx} = -y\frac{\partial \Phi}{\partial x}; \quad \epsilon_{xy} = \epsilon_{yx} = \frac{1}{2}\left(\frac{\partial u}{\partial x} - \Phi\right) \tag{2}$$

The total elastic strain energy is computed using the definition of strain energy density and the constitutive relations $\sigma_{xx} = E\epsilon_{xx}$ and $\sigma_{xy} = \sigma_{yx} = 2G\epsilon_{xy} = 2G\epsilon_{yx}$. Plugging into the energy and using the definitions of the strain components, we have

$$\Pi = \frac{1}{2}\int_v \sigma_{ij}\epsilon_{ij}dV = \frac{1}{2}\int_0^L \int_A E\epsilon_{xx}^2 + 4G\epsilon_{xy}^2 dA dx = \frac{1}{2}\int_0^L EI\left(\frac{\partial \Phi}{\partial x}\right)^2 + GA\left(\frac{\partial u}{\partial x} - \Phi\right)^2 dx \tag{3}$$

where $I = \int_A y^2 dA$ is the moment of inertia and A is the constant cross-sectional area. We have assumed implicitly that the shear strain is distributed evenly throughout the cross-section, which can be shown from equilibrium considerations to be incorrect. This assumption greatly simplifies analysis and can be improved with a shear correction factor κ. The correction factor multiplies the shear stiffness GA and depends on the cross-sectional geometry. Turning to the kinetic energy, we have

$$T = \frac{1}{2}\int_0^L \int_A \rho\left(\left(\frac{\partial u_x}{\partial t}\right)^2 + \left(\frac{\partial u_y}{\partial t}\right)^2\right) dA dx = \frac{1}{2}\int_0^L \rho I\left(\frac{\partial \Phi}{\partial t}\right)^2 + \rho A\left(\frac{\partial u}{\partial t}\right)^2 dx \tag{4}$$

Finally, the work of external forces $p(x,t)$ is simply

$$V = \int_0^L p(x,t)u(x,t)dx \tag{5}$$

The Lagrangian for the system is $\int T - \Pi - V dt$ where the strain energy now includes the shear correction κ. Combing Eqs. 3, 4 and 5 this reads

$$\mathcal{L} = \int_0^t \int_0^L -\frac{1}{2}EI\left(\frac{\partial \Phi}{\partial x}\right)^2 - \frac{1}{2}G\kappa A\left(\frac{\partial u}{\partial x} - \Phi\right)^2 - p(x,t)u(x,t) + \frac{1}{2}\rho I\left(\frac{\partial \Phi}{\partial t}\right)^2 + \frac{1}{2}\rho A\left(\frac{\partial u}{\partial t}\right)^2 dx dt \tag{6}$$

For a beam pinned on both ends, the displacement is zero and the rotation angle has zero derivative (no moment). Thus,

$$u(0) = u(L) = 0, \quad \frac{\partial \Phi}{\partial x}(0) = \frac{\partial \Phi}{\partial x}(L) = 0$$

Analytical solutions are possible to this problem, but are mathematically cumbersome and not amenable to uncertainty analysis [5]. Thus, using the Rayleigh-Ritz method, the spatial part of the displacement is naturally represented with the shape functions $\sin\left(\frac{\pi n}{L}x\right)$ and the spatial part of the rotation angle with $\cos\left(\frac{\pi m}{L}x\right)$ for $n, m = 1, 2, \ldots N$. With this choice of shape functions, the boundary conditions are satisfied automatically. The solution is approximated as

$$u(x,t) = \sum_n u_n(t)\sin\left(\frac{\pi n}{L}x\right) \tag{7a}$$

$$\Phi(x,t) = \sum_m \Phi_m(t)\cos\left(\frac{\pi m}{L}x\right) \tag{7b}$$

where the time-dependent coefficients $u_n(t)$ and $\Phi_m(t)$ are unknown. These expressions are substituted into the energy functional, the spatial integration is carried out, and the resulting expression is simplified to matrix-vector products. At this point, it is necessary to make assumptions about the material and geometric parameters in the energy. If some or all of these parameters are uncertain, do they vary in space? Or are they constant for a given beam but vary between parts? We will assume that the geometry of the beam is not uncertain, meaning that the area A, shear correction κ, and moment of inertia I are known and constant in space. The density will be treated as known and constant as well. In order to understand the interaction of an uncertain material and forcing, we will model the Young's modulus E as uncertain and spatially varying but the shear modulus G as known and constant. The problem will be driven by an applied load at an uncertain frequency with known magnitude. Furthermore, the load will be a point force at the center of the beam. Thus, we have $p(x,t) = p_0 \sin(2\pi f t)\delta(x - L/2)$ where f is the uncertain frequency. This kind of analysis could apply to a component near an engine which sees harmonic forcing over a range of frequencies. The designer wants to ensure that realistic variations in the material and uncertainty in the load frequency don't excite a resonance mode of the component. Carrying out the spatial integration, the Lagrangian can be written as

$$\mathcal{L} = \int \frac{1}{2}\dot{u}_i M^u_{ij}\dot{u}_j + \frac{1}{2}\dot{\Phi}_i M^\Phi_{ij}\dot{\Phi}_j + \Phi_i B_{ij} u_j - F_i u_i - \frac{1}{2}u_i U_{ij} u_j - \frac{1}{2}\Phi_i P_{ij}\Phi_j dt \tag{8}$$

$$M^u_{ij} := \frac{\rho A L}{2}\delta_{ij}$$

$$M^\Phi_{ij} := \frac{\rho I L}{2}\delta_{ij}$$

$$B_{ij} := \frac{G\kappa AL}{2}\left(\frac{\pi i}{L}\right)\delta_{ij}$$

$$F_i := p_0 \sin(2\pi f t)\sin\left(\frac{\pi i}{2}\right)$$

$$U_{ij} := \frac{G\kappa AL}{2}\left(\frac{\pi i}{L}\right)^2\delta_{ij}$$

$$P_{ij} := \left(\frac{\pi i}{L}\right)\left(\frac{\pi j}{L}\right)I\int_0^L E(x)\sin\left(\frac{\pi i}{L}x\right)\sin\left(\frac{\pi j}{L}x\right)dx + \frac{G\kappa AL}{2}\delta_{ij}$$

See the Appendix for detailed calculations. We now must use the Euler-Lagrange equations to determine the equations of motion corresponding to this action integral. The equations of motion are

$$M^u_{ij}\ddot{u}_j + U_{ij}u_j - B_{ij}\Phi_j = F_i$$

$$M^\Phi_{ij}\ddot{\Phi}_j + P_{ij}\Phi_j - B_{ij}u_j = 0$$

This can be re-written in block matrix form as

$$\begin{bmatrix} M^u & 0 \\ 0 & M^\Phi \end{bmatrix}\begin{bmatrix} \ddot{u} \\ \ddot{\Phi} \end{bmatrix} + \begin{bmatrix} U & -B \\ -B & P \end{bmatrix}\begin{bmatrix} u \\ \Phi \end{bmatrix} = \begin{bmatrix} F_i \\ 0 \end{bmatrix} \tag{9}$$

Collecting the coefficients on the displacement and rotation angle into a single vector unknown degrees of freedom, the above equation can be written as a generic undamped MDOF system:

$$M_{ij}\ddot{q}_j + K_{ij}q_j = f_i \tag{10}$$

where the mass and stiffness matrices are defined according to Eq. 9. We can now use the suite of techniques developed in the course to solve this coupled system of second-order ODE's. The vector q can be written with a spectral expansion as

$$q_i = \sum_r \eta_r(t)x_i^r \tag{11}$$

where the x_i^r are eigenvectors which the corresponding homogeneous eigenvalue problem

$$\left(K_{ij} - \omega_r^2 M_{ij}\right)x_j^r = 0$$

The eigenvectors are normalized and orthogonal with respect to the mass and stiffness matrices. Plugging this into the dynamical system and pre-multiplying by x_i^r, the orthogonality properties result in a decoupled system of ODE's:

$$\ddot{\eta}_r(t) + \omega_r^2\eta_r(t) = 0 \tag{12}$$

The choice of our shape functions in the Rayleigh-Ritz method was governed by the mathematically convenient pinned-pinned spatial boundary conditions. For simplicity, we now assume that the initial displacements and velocities are zero. This translates to

$$\eta_r(0) = \dot{\eta}_r(0) = 0 \tag{13}$$

These ODE's can be solved numerically or analytically and then be used to reconstruct the solution q, which is then used to compute the displacement and rotation angle for the beam. With a solver in hand, we would like to investigate the influence of uncertainty in problem parameters on quantities of interest such as maximum stress or displacement in the beam. In [6], a number of popular UQ techniques are reviewed. Chief among these are Monte Carlo methods and Polynomial Chaos Expansion (PCE). Monte Carlo methods require repeatedly sampling uncertain input parameters and obtaining solutions through the model. A distribution on the output is obtained after a large number of runs. Though PCE has the benefit of being less expensive, it is a more advanced UQ technique and is outside the scope of the class. Fortunately, the Timoshenko model is feasible to run a large number of times. Thus, we use Monte Carlo methods to quantify uncertainty in the dynamic Timoshenko beam from uncertain material and forcing. The quantity of interest that we will investigate is the maximum displacement over a given time interval.

IV. Results

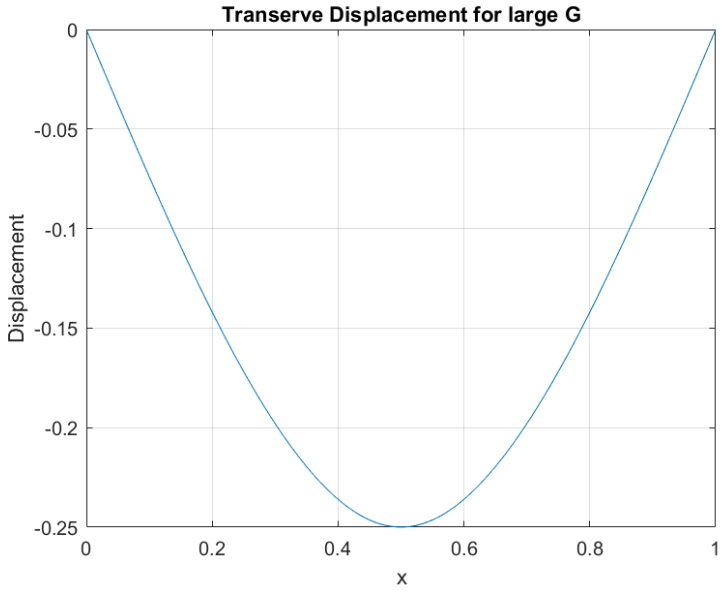

Fig. 3 The Timoshenko displacements from three-point test in the limit of $G \to \infty$ mimics that of the corresponding Euler beam.

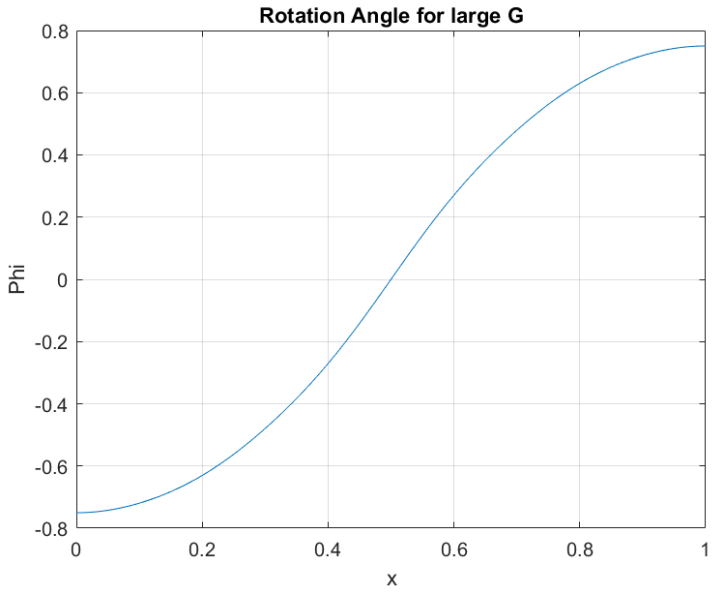

Fig. 4 The rotation angle for small shear deformations will approximate the derivative of the transverse displacement.

A. Code Verification

A MATLAB code is written to implement the solution procedure outlined above. Before proceeding to solve the random vibrations problem, we must first verify the equations have been implemented correctly. To do this, we will compare the Timoshenko code in a static three point bend to an Euler beam. The two should agree in the case of slender

Parameter	Value	Units
Nominal Young's Modulus (E_0)	1E7	Pa
Nominal Frequency (f_0)	1	rad/s
Shear Modulus (G)	2E6	Pa
Poisson Ratio (v)	0.3	–
Density (ρ)	2000	kg/m^3
Beam Length (L)	1	m
Cross-section Height (a)	0.1	m
Cross-section Depth (b)	0.1	m
Shear Correction (κ)	$\frac{10(1+v)}{11+12v}$	–
Load Magnitude (p_0)	1E3	N
Number of Shape Functions (N)	15	–

Table 1 Parameters and properties defining the problem.

cross-sectional geometry and/or large shear stiffness G. See Table 1 for a list of parameters used in the verification test and forthcoming analyses. A beam with square cross-section is analyzed, for which the shear correction factor is known and independent of the dimensions. We apply a point load p_0 at the center of the beam and observe the maximum displacement from the custom Timoshenko code and tabulated results from Euler beams with same boundary conditions and problem parameters. The Corresponding statics problem for the Timoshenko beam can be solved with

$$\underline{q} = \begin{bmatrix} u \\ \Phi \end{bmatrix} = \begin{bmatrix} U & -B \\ -B & P \end{bmatrix}^{-1} \begin{bmatrix} F \\ 0 \end{bmatrix}$$

from which the displacement coefficients u can be extracted and used to reconstruct the transverse deflection with Eq. 7. With a point load of $p_0 = 1000$ N applied at the center of the beam, pinned boundary conditions, and $E = 1E7$ Pa, an Euler beam obtains a maximum deflection of $u^E_{max} = 0.25m$. Using the parameters from Table 1, the max deflection of the Timoshenko beam is $u^T_{max} = 0.264m$. Timoshenko beams are less stiff, so it is logical the displacement is larger. However, we should obtain identical displacements when the shear stiffness goes to infinity, as the Timoshenko beam then reproduces the assumptions of the Euler model. When $G = 2E10$, the max displacement of the Timoshenko beam is $u^T_{max} = 0.249m$. Thus the model is working correctly, and we move on to more interesting analyses.

B. Monte Carlo Simulation of Random Vibrations

At each integration point, the Young's Modulus $E(x)$ will be distributed uniformly around a nominal value in the interval $E_0 \pm 0.15E_0$. This approximates a kind of spatial "white noise" distribution of the stiffness with maximum variations at 15% of the nominal value. Similarly, the frequency f will be distributed uniformly around a nominal in the interval $f_0 \pm 0.5f_0$. The frequency sweeps over a range of values in order to assess the forced response of the structure in an uncertain operating environment. We will run the dynamic analysis over a time period of $T = 10$ seconds, and extract the maximum displacement over this interval. This analysis is run 700 times to obtain a well-resolved Monte Carlo distribution of max displacements for sampled moduli and frequencies. See Figure 5 for the results of this analysis. The distribution is slightly skewed of max displacement below the average. The maximum displacement for the nominal material and forcing is $u_{max} = 0.426m$. When accounting for uncertainty in the forcing frequency and distribution of Young's Modulus, we see a range of ±25% variation around nominal in the max displacement. See Table 2 for summary statistics of the Monte Carlo distribution.

V. Conclusion

In this report, the kinematic assumptions of the Timoshenko beam were used to construct the Lagrangian from the kinetic and potential energies. The Rayleigh-Ritz was used along with simple boundary conditions to arrive a set of second order ODE's in time. A spectral expansion decoupled the system of equations, and the SDOF equations

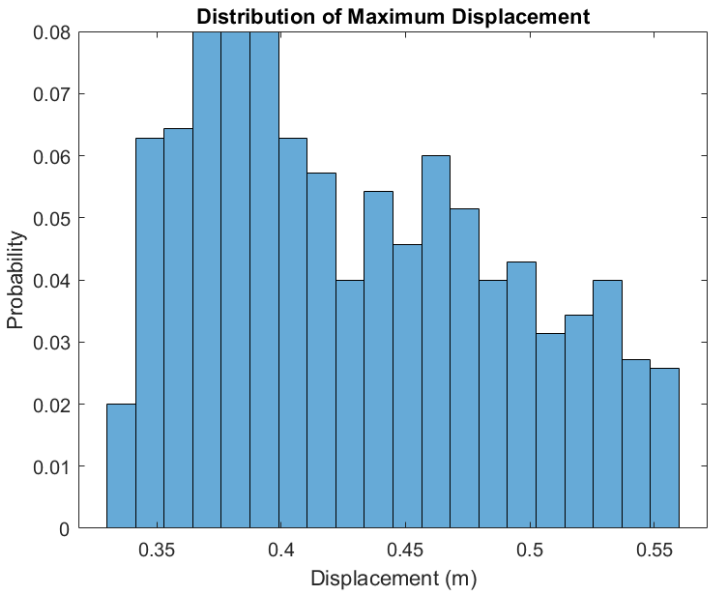

Fig. 5 Monte Carlo distribution for maximum bending displacement generated from 700 runs of randomly sampled forcing frequency and Young's Modulus distribution.

Statistic	Value
Mean	0.431
Standard Deviation	0.061

Table 2 Summary statistics of Monte Carlo distribution of 700 samples of max displacement. The average accurately matches the max displacement from nominal conditions and the standard deviation is approximately 15% **of the mean.**

were numerically integrated. This solver was used to analyze the impact of uncertainty in the beam material and applied forcing on the maximum bending displacement with Monte Carlo methods. It was shown that the Monte Carlo distribution was centered around the max displacement for nominal material/load conditions. For the specified distributions on the uncertain input parameters, the maximum displacement exhibited significant variability, thus demonstrating the need for uncertainty quantification in component design and analysis. If the designer needed to control the stiffness of the structure to avoid interfering with nearby parts, it would not suffice to run an analysis for the nominal values of inputs. Especially in dynamics problems, a structure's response can be very sensitive to small variations in inputs (resonance). Thus, it is essential to determine the degree of uncertainty in model inputs and quantify their impact on the system's response. As a final note, the Monte Carlo analysis is expensive even for the simple Timoshenko beam model. This demonstrates the importance of more efficient techniques like PCE.

Appendix–Energy Calculations

We look at different terms in the integrand of the Lagrangian one-by-one. The form of the solution is substituted and orthogonality of the shape functions is used to simplify expressions when possible. Recall that the spatial part of the Lagrangian is

$$\mathcal{L} = \int_0^L -\frac{1}{2}E(x)I\left(\frac{\partial\Phi}{\partial x}\right)^2 - \frac{1}{2}G(x)\kappa A\left(\frac{\partial u}{\partial x} - \Phi\right)^2 - p(x,t)u(x,t) + \frac{1}{2}\rho I\left(\frac{\partial\Phi}{\partial t}\right)^2 + \frac{1}{2}\rho A\left(\frac{\partial u}{\partial t}\right)^2 dx$$

The Young's Modulus E is uncertain and varies in space. The applied force $p(x,t)$ will be harmonic with an uncertain frequency.

Bending Strain Energy

$$-\int_0^L \frac{1}{2}E(x)I\left(\frac{\partial\Phi}{\partial x}\right)^2 dx = -\frac{1}{2}I\int_0^L E(x)\left(\sum_m \left(\frac{\pi m}{L}\right)\Phi_m(t)\sin\left(\frac{\pi m}{L}x\right)\right)\left(\sum_n \left(\frac{\pi n}{L}\right)\Phi_n(t)\sin\left(\frac{\pi n}{L}x\right)\right)dx$$

$$= -\frac{1}{2}I\sum_m\sum_n \left(\frac{\pi n}{L}\right)\left(\frac{\pi m}{L}\right)\Phi_n(t)\Phi_m(t)\int_0^L E(x)\sin\left(\frac{\pi m}{L}x\right)\sin\left(\frac{\pi n}{L}x\right)dx$$

$$\boxed{= -\frac{1}{2}\sum_m\sum_n \Phi_n(t)\Phi_m(t)\left[\left(\frac{\pi n}{L}\right)\left(\frac{\pi m}{L}\right)I\int_0^L E(x)\sin\left(\frac{\pi m}{L}x\right)\sin\left(\frac{\pi n}{L}x\right)dx\right]}$$

Shear Strain Energy

$$-\frac{1}{2}G\kappa A\int_0^L \left(\frac{\partial u}{\partial x}-\Phi\right)^2 dx = -\frac{1}{2}G\kappa A\int_0^L \left(\frac{\partial u}{\partial x}\right)^2 - 2\Phi\frac{\partial u}{\partial x}+\Phi^2 dx$$

Look at the three terms separately:

$$-\frac{1}{2}G\kappa A\int_0^L \left(\frac{\partial u}{\partial x}\right)^2 dx = -\frac{1}{2}G\kappa A\int_0^L \left(\sum_m \left(\frac{\pi m}{L}\right)u_m(t)\cos\left(\frac{\pi m}{L}x\right)\right)\left(\sum_n \left(\frac{\pi n}{L}\right)u_n(t)\cos\left(\frac{\pi n}{L}x\right)\right)dx$$

$$= -\frac{1}{2}G\kappa A\sum_m\sum_n \left(\frac{\pi m}{L}\right)\left(\frac{\pi n}{L}\right)u_m(t)u_n(t)\int_0^L \cos\left(\frac{\pi m}{L}x\right)\cos\left(\frac{\pi n}{L}x\right)dx$$

$$\boxed{-\frac{1}{2}\frac{G\kappa AL}{2}\sum_n \left(\frac{\pi n}{L}\right)^2 u_n(t)^2}$$

$$-\frac{1}{2}G\kappa A\int_0^L \Phi^2 dx = -\frac{1}{2}G\kappa A\int_0^L \left(\sum_m \Phi_m(t)\cos\left(\frac{\pi m}{L}x\right)\right)\left(\sum_n \Phi_n(t)\cos\left(\frac{\pi n}{L}x\right)\right)dx$$

$$\boxed{= -\frac{1}{2}\frac{G\kappa AL}{2}\sum_n \Phi_n(t)^2}$$

$$G\kappa A\int_0^L \Phi\frac{\partial u}{\partial x}dx = G\kappa A\int_0^L \left(\sum_m \Phi_m(t)\cos\left(\frac{\pi m}{L}x\right)\right)\left(\sum_n \left(\frac{\pi n}{L}\right)u_n(t)\cos\left(\frac{\pi n}{L}x\right)\right)dx$$

$$= G\kappa A\sum_m\sum_n \left(\frac{\pi n}{L}\right)\Phi_n(t)\Phi_m(t)\int_0^L \cos\left(\frac{\pi n}{L}\right)\cos\left(\frac{\pi m}{L}\right)dx$$

$$\boxed{= \frac{G\kappa AL}{2}\sum_n \left(\frac{\pi n}{L}\right)\Phi_n(t)u_n(t)}$$

Kinetic Energy

$$\frac{1}{2}\rho I \int_0^L \left(\frac{\partial \Phi}{\partial t}\right)^2 dx = \frac{1}{2}\rho I \int_0^L \left(\sum_n \frac{\partial \Phi_n}{\partial t}\cos\Big(\frac{\pi n}{L}x\Big)\right)\left(\sum_m \frac{\partial \Phi_m}{\partial t}\cos\Big(\frac{\pi m}{L}x\Big)\right)dx$$

$$= \frac{1}{2}\rho I \sum_m \sum_n \frac{\partial \Phi_m}{\partial t}\frac{\partial \Phi_n}{\partial t}\int_0^L \cos\Big(\frac{\pi n}{L}x\Big)\cos\Big(\frac{\pi m}{L}x\Big)dx$$

$$\boxed{= \frac{1}{2}\frac{\rho I L}{2}\sum_n \left(\frac{\partial \Phi_n}{\partial t}\right)^2}$$

$$\frac{1}{2}\rho A \int_0^L \left(\frac{\partial u}{\partial t}\right)^2 dx$$

$$\boxed{= \frac{1}{2}\frac{\rho A L}{2}\sum_n \left(\frac{\partial u_n}{\partial t}\right)^2}$$

Work of External Forces

The external force is applied as a point load with magnitude p_0 at the center of the beam which is harmonic in time.

$$= -\int_0^L u(x,t)p(x,t)dx = -\int_0^L u(x,t)p_0 \sin(2\pi f t)\delta(x - L/2)dx$$

$$= -p_0 \sum_n u_n \sin(2\pi f t)\int_0^L \sin\Big(\frac{\pi n}{L}x\Big)\delta(x - L/2)dx$$

$$\boxed{= -\sum_n u_n\Big(p_0 \sin(2\pi f t)\sin\Big(\frac{n\pi}{2}\Big)\Big)}$$

Appendix–Parameter Estimation

Assume that we have data for the trajectory of a damped Timoshenko beam pinned on both ends over S spatial points and T time points. We want to learn the damping matrix C which best fits the data. The objective function for this problem is

$$L = \frac{1}{2}\sum_{t=1}^{T}\sum_{s=1}^{S}\Big(u[t,s] - \hat{u}(t\Delta t, s\Delta x, C)\Big)^2$$

where minimizing the "loss" L corresponds to a best-fit damping matrix C. The quantity $u[t,s]$ represents the experimentally measured displacement at position $s\Delta x$ and time $t\Delta t$. Similar $\hat{u}$ is the prediction from the Timoshenko model which is a function of space, time, and the damping matrix C_{ij}. The gradient of the loss is

$$\frac{\partial L}{\partial C_{ij}} = \sum_t \sum_s -\Big(u[t,s] - \hat{u}(t\Delta t, s\Delta x, C)\Big)\frac{\partial \hat{u}}{\partial C_{ij}}$$

We need a method to compute the sensitivity of the prediction from the Timoshenko model w.r.t. the damping matrix in order to compute the gradient, which is used as the search direction in an iterative minimization scheme. We now turn to the underlying physical model to understand the computation of this sensitivity. A general damped dynamical system can be written as

$$M\ddot{q} + C\dot{q} + Kq = f$$

For the Timoshenko beam, q stores both the displacement and the rotation angle. We assume that the damping defined by matrix C is small, which implies that the eigenmodes for the damped vs. undamped system are approximately equivalent. Using the spectral representation of the solution, we can write

$$\underline{q} = \sum_r \eta_r(t)\underline{x}_r$$

Plugging this into the above equation, we find that

$$\ddot{\eta}_r + x_i^r C_{ij} x_j^r \dot{\eta}_r + \omega_r^2 \eta_r = 0$$

Here, x_i^r is the i-th component of eigenmode r. We obtain de-coupled normal equations as a result of the small damping assumption. The displacement prediction from the pinned-pinned Timoshenko model approximated with global shape functions is

$$\hat{u}(x,t) = \sum_{n=1}^{N} q_n \sin\Big(\frac{n\pi}{L}x\Big)$$

where N is the number of shape functions used in the approximation. Note that the dimension of q is $2N$. Plugging in the spectral representation for q, this becomes

$$\hat{u}(x,t) = \sum_{n=1}^{N} \Big(\sum_{r=1}^{2N} \eta_r(t) x_n^r \Big) \sin\Big(\frac{n\pi}{L}x\Big)$$

Then the sensitivity can be written as

$$\frac{\partial \hat{u}(x,t)}{\partial C_{ij}} = \sum_{n=1}^{N} \Big(\sum_{r=1}^{2N} \frac{\partial \eta_r(t)}{\partial C_{ij}} x_n^r \Big) \sin\Big(\frac{n\pi}{L}x\Big)$$

This is because the spatial shape functions and eigenmodes do not depend on the damping. Thus in order to compute the sensitivity of the solution, we need to compute sensitivities of the normal equations as the spatial shape functions and eigenmodes are unchanged. We can differentiate the normal equations w.r.t the damping

$$\frac{\partial \ddot{\eta}_r}{\partial C_{ij}} + x_k^r C_{k\ell} x_\ell^r \frac{\partial \dot{\eta}_r}{\partial C_{ij}} + x_k^r \frac{\partial C_{k\ell}}{\partial C_{ij}} x_\ell^r \dot{\eta}_r + \omega_r^2 \frac{\partial \eta_r}{\partial C_{ij}} = 0$$

This can be rewritten as a second-order ODE for the matrix of sensitivities

$$\frac{\partial^2}{\partial t^2}\left(\frac{\partial \eta_r}{\partial C_{ij}}\right) + x_k^r C_{k\ell} x_\ell^r \frac{\partial}{\partial t}\left(\frac{\partial \eta_r}{\partial C_{ij}}\right) + \omega_r^2 \left(\frac{\partial \eta_r}{\partial C_{ij}}\right) = -x_i^r x_j^r \dot{\eta}_r$$

The eigenfrequencies ω_r do not depend on the damping and the term $\dot{\eta}_r$ is known from the solving the system at the current damping matrix. For each η_r, we need to solve a series of ODE's for different forcings and then pass this solution back through the spectral expansion and displacement approximations in order to compute sensitivities. With this in hand, the gradient can be evaluated and used a search direction to look for a minimum to the loss function. This process fits a damping matrix under the small damping assumption which optimally reproduces the experimental when used in the Timoshenko model.

References

[1] "Timoshenko–Ehrenfest Beam theory," Wikipedia Available: https://en.wikipedia.org/wiki/Timoshenko%E2%80%93Ehrenfest_beam_theory.

[2] Guo, S., "Uncertainty quantification explained," Medium Available: https://towardsdatascience.com/managing-uncertainty-in-computational-science-and-engineering-5e532085512b.

[3] Sudret, B. (2014) Polynomial chaos expansions and stochastic finite element methods, Risk and Reliability in Geotechnical Engineering (Chap.6), pp.265-300, CRCPress.

[4] Bauchau, O. A., and Craig, J. I., "Shearing Deformation in Beams," Structural Analysis: With Applications to Aerospace Structures, Springer, 2009, pp. 793–814.

[5] van Rensburg, N. F. J., and van der Merwe, A. J., "Natural frequencies and modes of a timoshenko beam," Wave Motion, vol. 44, 2006, pp. 58–69.

[6] Kumar, D., Ahmed, F., Usman, S., Alajo, A., and Alam, S. B., "Recent advances in uncertainty quantification methods for engineering problems," AI Assurance, 2023, pp. 453–472.